ELSEVIER

Journal of Nuclear Materials 307–311 (2002) 1112–1119

journal of nuclear materials

www.elsevier.com/locate/jnucmat

Optimizing the transverse thermal conductivity of 2D-SiC_f/SiC composites. I. Modeling

G.E. Youngblood *, D.J. Senor, R.H. Jones

Pacific Northwest National Laboratory, MS-K2-44, Battelle Boulevard, Richland, WA 99352, USA

Abstract

For potential fusion energy applications, considerable fabrication efforts have been directed to obtaining transverse thermal conductivity (K_{eff}) values in excess of 30 W/m K (unirradiated) in the 800–1000 °C temperature range for 2D-SiC_f/SiC composites. To gain insight into the factors affecting K_{eff}, at PNNL we have tested three different analytic models for predicting K_{eff} in terms of constituent (fiber, matrix and interphase) properties. The tested models were: the Hasselman–Johnson '2-Cylinder' model, which examines the effects of fiber–matrix (f/m) thermal barriers; the Markworth '3-Cylinder' model, which specifically examines the effects of interphase thickness and thermal conductivity; and a newly developed anisotropic '3-Square' model, which examines the potential effect of introducing a fiber coating with anisotropic properties to enhance (or diminish) f/m thermal coupling. The first two models are effective medium models, while the third model is a simple combination of parallel and series conductances. Model predictions suggest specific designs and/or development efforts directed to optimize the overall thermal transport performance of 2D-SiC_f/SiC.

1. Introduction

Many potential applications of continuous fiber-reinforced ceramic composites (CFCC) require relatively high thermal conductivity. This study will focus on the conditions for optimizing the transverse thermal conductivity (K_{eff}) of a CFCC, consisting of a silicon carbide (SiC) matrix reinforced with SiC-type fibers (SiC_f), for potential fusion reactor applications. Usually the SiC matrix is made by using the chemical vapor infiltration (CVI) process, but polymer infiltration and pyrolysis (PIP) and hybrid CVI–PIP processes also are being developed [1].

Recently, the design goal for a fusion reactor SiC_f/SiC first wall was set at 15 W/m K at 800 °C in service [2]. This translates roughly into a goal for unirradiated SiC_f/SiC to have $K_{eff} = 38$ W/m K at 800 °C, which is a value about three times that reported for even the best, currently available commercial 2D-SiC_f/SiC [3]. To attain a high K_{eff}, both the fiber and matrix components will have to have relatively high thermal conductivity values, K_f and K_m, respectively. The fiber type likely will be highly crystallized, stoichiometric SiC with $K_f > K_m$. Moreover, good fiber–matrix (f/m) thermal coupling will be required.

To investigate the separate component contributions to K_{eff}, three different analytic models were examined, namely: (1) the Hasselman–Johnson (H–J) '2-Cylinder' model [4], (2) the Markworth '3-Cylinder' model [5], and (3) a newly developed '3-Square' model with anisotropic thermal conduction. The validity, limiting conditions and appropriate circumstances for using each model will be discussed. To test the models, predictions are compared to experimental measurements of K_{eff} for a commercial SiC_f/SiC system and presented in a companion paper [6]. Model descriptions follow:

1.1. The Hasselman–Johnson model

The H–J model is an effective medium (EM) model that describes steady-state heat transport in the transverse

* Corresponding author. Tel.: +1-509 375 2314; fax: +1-509 375 2186.

E-mail address: ge.youngblood@pnl.gov (G.E. Youngblood).

0022-3115/02/$ - see front matter
PII: S0022-3115(02)00951-0

direction in a composite with dispersed, uniaxially aligned fibers. It predicts K_{eff} in terms of K_{f} and K_{m}, the fiber diameter, the average fiber volume fraction (f) and the effects of f/m thermal barriers. Predictions of K_{eff} for such a composite have been shown to be in close agreement ($\leqslant 5\%$) with detailed finite element model predictions for f-values up to $f \leqslant 0.5$ [7].

In the EM approach, attention is focused on a single fiber aligned coaxially within a cylindrical matrix which itself is contained within an effectively homogeneous EM, as schematically depicted in Fig. 1(a). The EM stretches to infinity and represents the average effect of all the surrounding fibers and matrix material outside the two inner cylinders. The inner fiber and matrix cylinders have cross-sectional radii a and b, respectively. The magnitude of the radius b is set by the requirement that the fiber volume fraction $f = a^2/b^2$. A temperature gradient (ΔT), which is uniform throughout the EM, is directed along the positive x-direction. Because of the cylindrical geometry, the temperature distributions in each region i ($i = 1$, 2, 3 or eff, m, f, respectively) are assumed to have the general form:

$$T_i = A_i + (B_i/\rho + C_i\rho)\cos(\theta), \tag{1}$$

where ρ and θ are the usual cylindrical polar coordinates. The values for the constants A_i, B_i and C_i are obtained by applying the boundary conditions that the normal component of heat flux $K_i(\mathrm{d}T_i/d\rho_n)_n$ be continuous across each interface at $\rho = a$ or b, and that $T_{\text{m}} = T_{\text{eff}}$ at the matrix–EM interface $\rho = b$. At the f/m interface $\rho = a$, a finite temperature step $T_{\text{f}} - T_{\text{m}} = -K_{\text{f}}/h(\mathrm{d}T_{\text{f}}/d\rho)_n$ is introduced. The f/m interface conductance is represented by 'h' and has units of W/m^2 K. The goal is to derive an expression for K_{eff} in terms of K_{f}, K_{m}, a, f, and h.

Since the temperature scale is arbitrary, A_3 can be set to zero; and since the temperature must be finite at the origin, $B_3 = 0$. By symmetry about the mid-plane perpendicular to the temperature gradient, A_2 and A_1 must also be zero. Finally, for T_{eff} to vary uniformly along the temperature gradient within the EM region, $B_1 = 0$ and $C_1 = \Delta T$. Applying the boundary conditions at both $\rho = a$ and b, one obtains a system of four coupled equations containing three unknown terms, B_2, C_2 and C_3:

$$C_2 - B_2/a^2 = rC_3, \tag{2a}$$

$$C_2 + B_2/a^2 = (x+1)C_3, \tag{2b}$$

$$C_2 - B_2/b^2 = R\Delta T, \tag{2c}$$

$$C_2 + B_2/b^2 = \Delta T, \tag{2d}$$

where the substitutions $r = K_{\text{f}}/K_{\text{m}}$, $R = K_{\text{eff}}/K_{\text{m}}$ and $x = K_{\text{f}}/ah$ have been used to simplify the algebra. By adding or subtracting Eqs. (2c) and (2d), separate solutions for C_2 and B_2 can be derived in terms of b^2, R and ΔT. Then by substituting the solutions for C_2 and B_2 into both Eqs. (2a) and (2b), two independent expressions for C_3 are obtained. Setting these two expressions equal to each other and using the requirement that $f = a^2/b^2$, it is straightforward to solve for R obtaining:

$$R = \{(r+x+1) + f(r-x-1)\} / \{(r+x+1) - f(r-x-1)\}. \tag{3}$$

Eq. (3) is the same equation derived by Hasselman and Johnson by a similar method. To simplify the analysis, we have normalized both K_{eff} and K_{f} by dividing by K_{m} and we have introduced the quantity x, which is the reciprocal of the Biot number or the surface heat transfer coefficient. Note that the EM method works because the four coupled equations with three

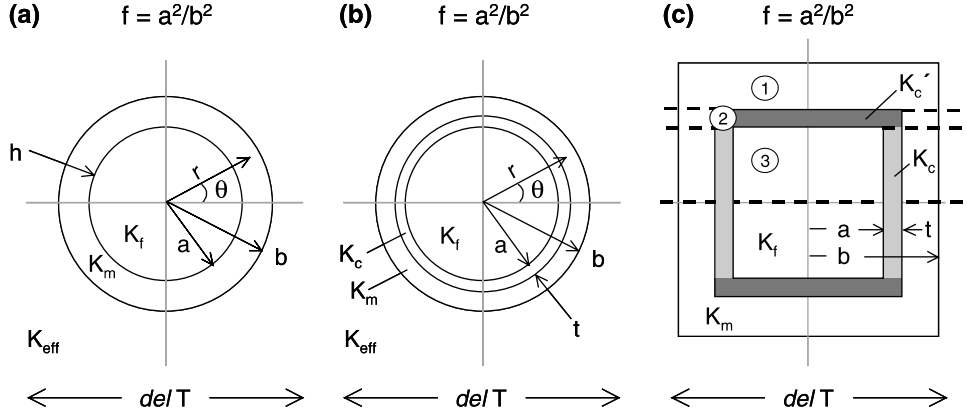

Fig. 1. Schematic cross-sectional views of fiber/interface/matrix geometry for (a) H–J 2-Cylinder model, (b) the Markworth 3-Cylinder model, and (c) the anisotropic 3-Square model.

unknowns overspecify the situation, which permits the analytic solution for R (or K_{eff}).

In Fig. 2(a) and (b), the relative thermal conductivity R is plotted as a function of 'h' for fiber volume fractions $f = 0.1$, 0.4, 0.5 and 0.6 for two different f/m conductivity ratios, $r = 5$ and 0.2. To easily compare the effects of r and h on K_{eff} for these examples, the same fiber radius and matrix thermal conductivity ($a = 5$ μm and $K_{\text{m}} = 20$ W/m K, respectively) were assigned. The following observations are made:

(1) As $f \to 0$ (e.g., $f = 0.1$), $R \to 1$ for all values of h (and r).
(2) For $r > 1$, R is sensitively dependent on h and there is a common crossover point at $R = 1$ for all values of f when $x = r - 1$.
(3) For $r < 1$, R is relatively insensitive to the values of h, there is no crossover point and $R < 1$ for all values of f and h.
(4) For $h \to 0$ (complete f/m thermal decoupling), R asymptotically approaches a minimum value independently of r given by $R_{\text{min}} = (1 - f)/(1 + f)$.
(5) For $h \to \infty$ (perfect f/m thermal coupling), R asymptotically approaches a maximum value which is given by $R_{\text{max}} = [(1 - f) + r(1 + f)]/[(1 + f) + r(1 - f)]$.

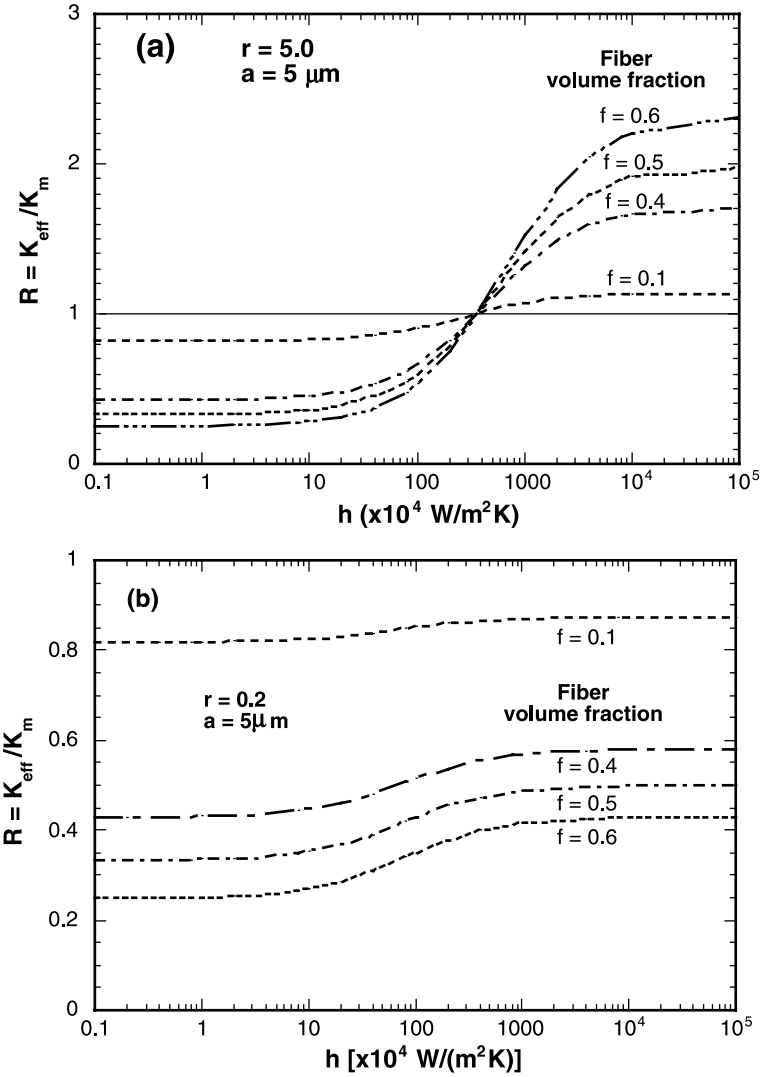

Fig. 2. Comparison of analytic solutions for the H–J equation (3), R versus h for fiber volume fractions up to $f = 0.6$ for $K_{\text{f}}/K_{\text{m}}$ ratios (a) $r = 5.0$ and (b) $r = 0.2$. For each case, the fiber radius $a = 5.0$ μm and $K_{\text{m}} = 20$ W/m K.

(6) For ($r < 1$), as r increases the transition region (the region where R exhibits its maximum rate of change) occurs for lower (higher) values of h.

Clearly, for dispersed parallel fibers in a matrix, K_{eff} is controlled primarily by the continuous matrix phase thermal conductivity, K_{m}. To attain a K_{eff}-value greater than K_{m}, both relatively high K_{f}- and h-values are necessary. Even when $r = 100$, by observation (5) for a typical SiC_f/SiC fiber packing fraction $f = 0.4$, $R_{\max}$ would still be <2.3 for perfect f/m thermal coupling. At the other extreme, when $h \to 0$ the fibers become thermally decoupled from the matrix and $R_{\min}$ is representative of the limiting case for dispersed cylindrical pores with a volume fraction 'f'. This latter point has important consequences for SiC_f/SiC designed to have a high K_{eff}, i.e., for a composite made from matrix and fibers with individually high K-values as well as with originally high conductance interfaces. For this example, degradation of the interface alone ($h \to 0$), due possibly to mechanical, thermal or environmental stress, is sufficient for $K_{\text{eff}}/K_{\text{m}}$ to be reduced from a maximum value of 2.3 down to a minimum value of 0.42, an 82% reduction! Independent degradation of K_{m} could further reduce K_{eff}.

1.2. The Markworth model

The Markworth model also is an EM model in which the f/m interface shown in Fig. 1(a) is replaced by a thin fiber coating of thickness (t) and thermal conductivity (K_{c}), as shown in Fig. 1(b) [5]. The temperature distribution given by Eq. (1) again is assumed; and the boundary conditions now are applied between four separate regions rather than three, where the outer region again is the EM with temperature gradient ΔT and an effective thermal conductivity K_{eff}. There no longer is a temperature step at the f/m interface, but T_i and $K_i(\mathrm{d}T/\mathrm{d}\rho)_n$ are continuous at the three interfaces between the four regions. The result is a set of six coupled equations with five unknown coefficients. Again, the overspecification of the unknown coefficients permits a unique solution for R (or K_{eff}), specifically:

$$R_{3\text{cyl}} = f(K_{\text{m}}, K_{\text{c}}, K_{\text{f}}; f, t, a)/g(K_{\text{m}}, K_{\text{c}}, K_{\text{f}}; f, t, a), \tag{4}$$

where $R_{3\text{cyl}} = K_{\text{eff}}/K_{\text{m}}$ for the Markworth [1] or 3-Cylinder model and the functions f and g are given by

$$f = 2c(r+c)[1 + f(1+u)^2] + [(c-1) + f(1+u)^2 \times (c+1)][(r-c)/(1+u)^2 - (r+c)], \tag{5}$$

$$g = 2c(r+c)[1 - f(1+u)^2] + [(c-1) - f(1+u)^2 \times (c+1)][(r-c)/(1+u)^2 - (r+c)]. \tag{6}$$

Eqs. (5) and (6) are normalized by setting $u = t/a$ and $c = K_{\text{c}}/K_{\text{m}}$, and $r = K_{\text{f}}/K_{\text{m}}$ as before. If c is set = 0 (equivalent to $K_{\text{c}} = 0$ for perfectly insulated fibers), Eq. (4) reduces to the limit:

$$R_{3\text{cyl}}(\min) = [1 - f(1+u)^2]/[1 + f(1+u)^2], \tag{7}$$

which is equivalent to the limiting condition for $R_{\min}$ given by observation (4) for the H–J model. If u is set = 0 (equivalent to no coating), an upper limit for $R_{3\text{cyl}}$ becomes:

$$R_{3\text{cyl}}(\text{no coat}) = [(1-f) + r(1+f)]/[(1+f) + r(1-f)], \tag{8}$$

which is the same as the limiting condition given by observation (5) when $h \to \infty$ (perfect f/m thermal coupling) for the H–J model. However, Eq. (8) does not represent an upper bound for $R_{3\text{cyl}}$. For a high value of c (or K_{c}), by Eq. (4) $R_{3\text{cyl}}$ continuously increases as t increases.

In Fig. 3(a), $R_{3\text{cyl}}$ is plotted versus an equivalent conductance ($h_{\text{eq}} = K_{\text{c}}/t$) so that solutions for the 3-Cylinder model can easily be compared to solutions for the H–J model for the same K_{f}^--, K_{m}^-- and a-values. For the case of $K_{\text{f}} = 100$ W/m K and $K_{\text{m}} = 20$ W/m K, the curves for equivalent f-values have similar S-shapes with a crossover where $R = 1.0$ for all values of 'f'. However, $R_{3\text{cyl}} > R$ for $h_{\text{eq}} > 10^7$ W/m^2 K. This is because a fiber coating with a high K_{c}-value relative to K_{m} begins to contribute to K_{eff}. This effect becomes more pronounced as the coating thickness increases, as is shown in Fig. 3(b) for a case where $f = 0.6$. For instance, if $K_{\text{c}} = 1000$ W/m K and $t/a = 0.14$ (e.g., a 14-μm diameter fiber with a coating 1-μm thick) $R_{3\text{cyl}} \approx 4.7$, a value more than twice as much as the upper limit when the coating is infinitely thin. Obviously, for cases where a fiber has a relatively thick coating with a high K_{c}, the coating itself can contribute significantly to K_{eff}. In contrast, if the fiber coating is insulating (e.g., a layer of amorphous SiO_2) $R_{3\text{cyl}}$ rapidly becomes <1.0 as t increases, and approaches the lower limit set by Eq. (7). As an example, if $K_{\text{f}} = 100$ W/m K, $K_{\text{m}} = 20$ W/m K, $f = 0.6$ and $K_{\text{c}} = 0.1$ W/m K, $R_{3\text{cyl}} \to \approx 0.25$ for $t/a > 0.04$.

1.3. The anisotropic 3-Square model

Both the H–J 2-Cylinder and the Markworth 3-Cylinder models assume that all the constituents are transversely isotropic. However, commonly used pyrolytic carbon (PyC) fiber coatings generally have a turbostratic texture in which the carbon a-axis (the high thermal

[1] In Ref. [5], errors appear in Eqs. (10) and (14), the expressions for R and g. In Eq. (14), the last two minus signs should be replaced by multiplication signs; and in Eq. (14), the term $[1 + \lambda(1+\mu)^2]$ should be $[1 - \lambda(1+\mu)^2]$.

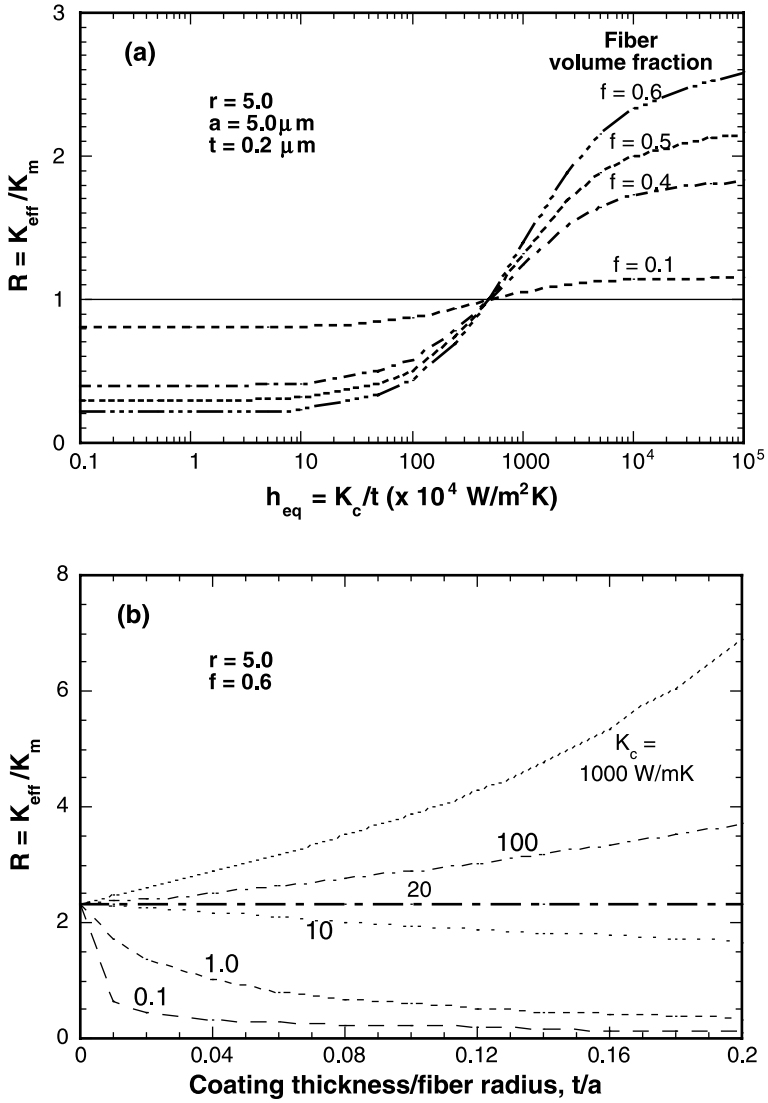

Fig. 3. Comparison of analytic solutions for the Markworth model equation (4) for $K_f/K_m = 5.0$, $K_m = 20$ W/m K and $a = 5.0$ μm. (a) R versus $h_{eq} = K_c/t$ for fiber volume fractions up to $f = 0.6$ and $t = 0.2$ μm, and (b) R versus t/a for $K_c = 0.1$ up to 1000 W/m K.

conductivity direction for graphite) is preferentially aligned parallel and the low-conductivity c-axis perpendicular to the fiber surface [8]. For this reason, a simple model was developed to examine the effect of anisotropic thermal conduction in the fiber coating. In this model, rather than concentric cylinders the configuration consists of three concentric bars with square cross-sections representing the fiber, fiber coating and matrix phases, as schematically depicted in Fig. 1(c). The bars are subdivided into symmetric regions 1, 2 and 3 with respect to their common central plane. For simplicity, no lateral heat conduction is allowed between the regions. Then K_{eff} for this system becomes a combination of series and parallel conductances for each of the three regions:

$$K_{eff} = F_1(K_m; b, a, t) + F_2(K_m, K_{c'}; b, a, t) + F_3(K_m, K_c, K_f; b, a, t), \quad (9)$$

where the conductance contribution from each region is given explicitly by

$$F_1(K_m; b, a, t) = K_m[1 - (a + t)/b], \quad (9a)$$

$$F_2(K_m, K_{c'}; b, a, t) = K_m[(b - a)/t - 1 + (K_m/K_{c'})(t + a)/t]^{-1}, \quad (9b)$$

$$F_3(K_m, K_c, K_f; b, a, t) = K_m[(b-t)/a - 1 + (K_m/K_c)(t/a) + K_m/K_f]^{-1}. \quad (9c)$$

In Eqs. (9a)–(9c), the contributions from regions 1, 2 and 3 contain conductances for the matrix only; matrix and fiber coating in series; and matrix, fiber coating and fiber in series, respectively.

Because the thermal conductivity of graphite exhibits an extremely wide range between maximum and minimum values (2000 and 10 W/m K parallel and normal to the basal c-planes, respectively), even a small component of in-plane conductivity can significantly affect K_c. As an example, predictions for K_{eff} as a function of t/a are presented in Fig. 4(a) and (b) for the 3-Square model when the coating has two different types of texture. For this example, values of $K_{c(a)}$ and $K_{c(c)}$ were selected to be 500 and 2 W/m K, respectively. Also, for ease of comparison to the 3-Cylinder model example (Fig. 3(b) the same values for K_m and K_f, equivalent fiber radius a, and $f = a^2/b^2 = 0.6$ were selected for the 3-Square model example.

The three lower curves in each of Fig. 4(a) and (b) represent the separate contributions of the three parallel conduction pathways F_1, F_2 and F_3 while the upper solid

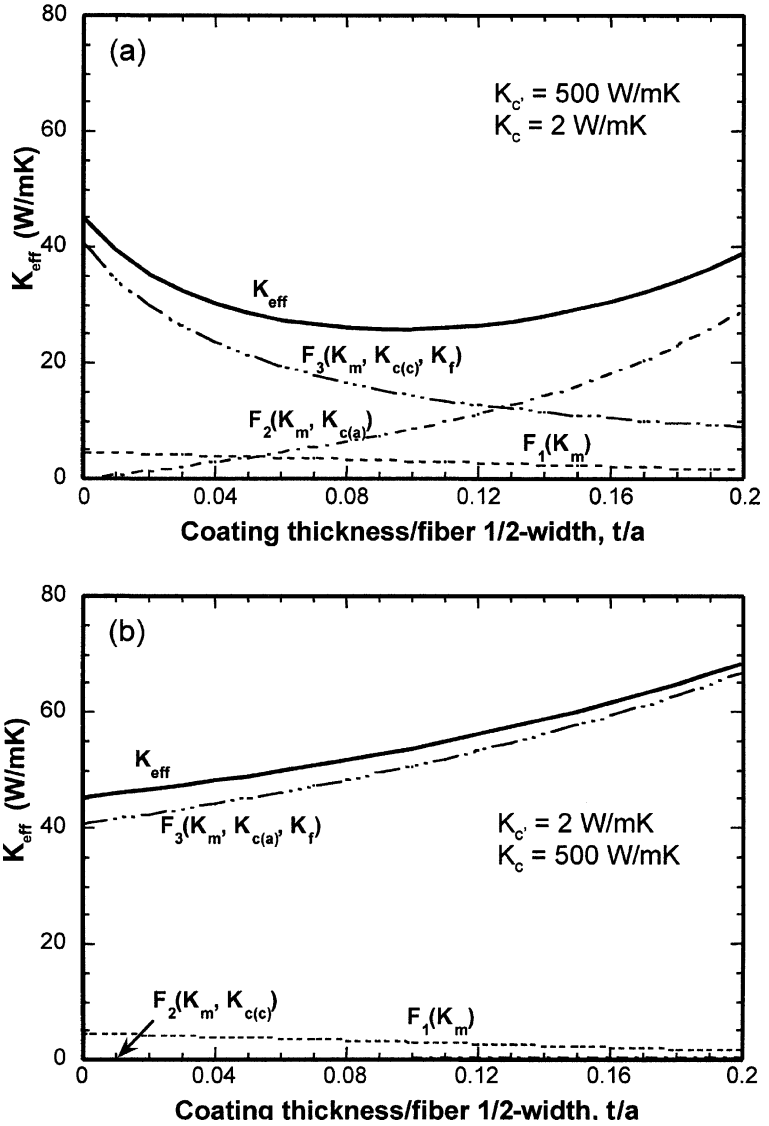

Fig. 4. Comparison of analytic solutions for the anisotropic 3-Square model equation (9) for $K_f/K_m = 5.0$, $K_m = 20$ W/m K, $a = 5.0$ μm and $f = 0.6$ when (a) $K_{c'} = K_{c(a)} = 500$ W/m K and $K_c = K_{c(c)} = 2$ W/m K, or when (b) $K_{c'} = K_{c(c)} = 2$ W/m K and $K_c = K_{c(a)} = 500$ W/m K.

curve (the algebraic sum of the three lower curves) represents K_{eff}. In Fig. 4(a), the coating texture is such that heat conduction within the coating along the edges of the fiber (region 2) is enhanced by the alignment of the high-conductivity PyC a-axis parallel to ΔT. Meanwhile, in region 3 the alignment of the low-conductivity c-axis parallel to ΔT tends to insulate the fiber from the matrix. At the other extreme, in Fig. 4(b) the coating texture is such that alignment of the low-conductivity c-axis is preferentially parallel to ΔT in region 2, which reduces heat conduction in the coating along the edges of the fiber. Then, in region 3 the high-conductivity a-axis is parallel to ΔT so that the fiber is thermally well coupled to the matrix.

In Fig. 4(a), K_{eff} exhibits a minimum value because the f/m coupling curve (F3) decreases and the fiber coating shorting curve (F2) increases as t increases. For this selected case, the minimum occurs for $t/a = 0.085$. Then, for a fiber with equivalent diameter 10 μm, $t > 400$ nm. The matrix only contribution (F1) is relatively small and decreases slightly with increasing t simply because of a decrease in the cross-sectional area for region 1. Obviously, the F1 contribution would increase somewhat for values of $f < 0.6$.

In contrast, when the fiber is effectively coupled to the matrix through the F3 term, K_{eff} continuously increases with increasing t and the fiber shorting contribution F2 is nearly non-existent, as depicted in Fig. 4(b). For this case, the coating texture is such that little heat conduction occurs in the coating along the edges of the fiber parallel to ΔT because of the low value selected for $K_{c(c)}$. However, the fiber is thermally well coupled to the matrix because of the high value selected for $K_{c(a)}$. Also, for this example with $f = 0.6$ the region 3 cross-section is relatively high compared to either of the cross-sections for regions 1 or 2.

2. Discussion

The H–J 2-Cylinder and the Markworth 3-Cylinder models are similar EM models whose thermal transport predictions depend upon the composite constituent (fiber, fiber coating, and matrix) dimensions, thermal properties and their arrangement as well as the actual character of the different interfaces between these constituents. Similar predictions of R are obtained for similar values of h or equivalent $h_{\text{eq}} = K_c/t$ for the H–J and Markworth models, respectively. The only difference is that the Markworth model predicts higher values for R when $h_{\text{eq}} > 10^7$ W/m^2 K because then the coating also begins to contribute to K_{eff}. Therefore, to describe well-bonded SiC$_f$/SiC systems with high values of h_{eq} the Markworth model is preferred, while the H–J model is preferred when debonding and/or numerous f/m gas gaps occur which dominate the interfacial conductance and result in relatively low h-values.

Percolation effects through direct fiber–fiber contacts and through the inner-connected PyC coatings likely will enhance K_{eff}. Such effects will become more important as the number of contacts and inner-connections increase either as the average 'f' increases or as the fiber packing within individual tows increases locally, as observed for most 2D-SiC$_f$/SiC systems made from woven fabric layers. Also, K_{eff} will increase as the K_c-values increase, especially if the coating thickness also increases. Nevertheless, relative changes in predicted K_{eff}-values should be little affected by moderate distortions in the theory due to fiber packing non-uniformity or percolation effects.

Constituent properties, K_f, K_m, K_c (or h), sometimes can be measured independently in a simulated system. However, they may not be representative of the quantities as they exist in an actual composite because the composite processing conditions are difficult to reproduce. A better way to estimate the individual constituent properties is to use either the H–J or the Markworth models to estimate constituent quantities from measured values of K_{eff} and structural data. To extract values of K_m and K_c (or h) from models, accurate K_{eff} data must be obtained as a function of other variables, e.g., fiber radius and volume content, and coating thickness. If the temperature dependence of K_m, K_c (or h) is known or can reliably be estimated, measuring K_{eff} as a function of temperature also is a useful strategy. Furthermore, if K_{eff} for composites exposed to irradiation or other treatments can be modeled, a detailed analysis of degradation mechanisms may be possible by separately estimating the degradation effects for the individual constituents.

In the H–J model, K_{eff} can be affected by the size of the fibers (or particulate) through the K_f/ah term. For instance, attempts have been made to improve K_{eff} by adding high thermal conductivity diamond or SiC particulate to cordierite or aluminum substrates, at the same time toughening or strengthening these substrates. In these cases, the h-values were quite high ($h > 10^7$ W/m^2 K). However, this strategy failed due to the small sizes of the diamond or SiC particulate used. Rather than making a contribution to K_{eff}, the smaller particulates acted more like insulating voids because of a size effect where a small a-value offsets the benefit of a large h-value. A size-effect could reduce K_{eff} for a composite reinforced by SiC fiber with a high K_f, but also a small diameter. The H–J model is particularly appropriate to analyze this situation for most cases.

Finally, the anisotropic 3-Square model suggests a design strategy that may further enhance K_{eff} for composites with PyC fiber coatings. To take advantage of a fiber with a high K_f-value, the fiber must be thermally well coupled to the matrix. To do this, perhaps the

texture of a PyC coating can be controlled to better provide such coupling. The texture would need to preferentially align the high-conductivity PyC a-axis normal to the fiber surface, not parallel to the surface as is typically observed [8]. Also, the PyC coating possibly could be further graphitized to enhance its K_c-value. However, this latter strategy would work only if the coating texture could also be controlled, or at least maintained isotropic.

3. Summary

1. The H–J 2-Cylinder and the Markworth 3-Cylinder models are useful for designing 2D-woven SiC_f/SiC composites with a high K_{eff}-value or for analyzing K_{eff} to obtain individual constituent K_m, K_c (or h) values.
2. For composite with debonds or delaminations, the H–J model is preferred for analysis. For composite with a uniform fiber coating and with well-bonded f/c/m interfaces, the Markworth model is preferred.
3. To achieve high K_{eff}, SiC_f/SiC composite must first have a high K_m-value, then also a high K_f-value with high h or h_{eq}-values.
4. The anisotropic nature of K_c for a PyC fiber coating may be utilized to improve (or degrade) h_{eq}, and thus improve or degrade the overall composite K_{eff}.
5. Even for a composite with well-bonded f/m interfaces, a size effect may reduce K_{eff} if the fibers have too small a diameter.

Acknowledgements

This work was supported by the US Department of Energy under the Nuclear Energy Research Initiative (NERI) program. The Pacific Northwest National Laboratory is operated by Battelle Memorial Institute for the US Department of Energy under contract DE-AC 06-76RLO 1830.

References

[1] W. Kowbel, A. Tsou, C. Bruce, J.C. Withers, G.E. Youngblood, these Proceedings.
[2] R. Jones, in: Performance requirements for structural applications of SiC/SiC, Proceedings for the 1st IEA International Workshop on SiC/SiC Ceramic Composites for Fusion Structural Applications, 28–29 October 1996, Ispra (Va), Italy, p. 196.
[3] D.J. Senor, G.E. Youngblood, D.V. Archer, C.E. Chamberlin, Recent progress in thermal conductivity testing of SiC-based materials for fusion reactor applications, Proceedings of the 3rd IEA Workshop on SiC/SiC Ceramic Composites for Fusion Structural Applications, January 29–30, 1999, Cocoa Beach, FL, p. 102.
[4] D.P.H. Hasselman, L.F. Johnson, J. Mater. Sci. Lett. 10 (1991) 682.
[5] A.J. Markworth, J. Mater. Sci. Lett. 12 (1993) 1487.
[6] G.E. Youngblood, D.J. Senor, R.H. Jones, Witold Kowbel, Companion paper.
[7] S. Graham, Ph.D. thesis, Chapter 5, Random geometry influences on effective thermal conductivity, Georgia Institute of Technology, Atlanta, GA, 1999.
[8] C. Labrugere, A. Guette, R. Naslain, J. Eur. Ceram. Soc. 17 (1997) 623.